Jewel Journal of Scientific Research (JJSR) 10(2): 364–373, 2025
©Federal University of Kashere-Nigeria (Print ISSN: 2384 – 6267, Online ISSN 2756-651X)
https://journals.fukashere.edu.ng/index.php/jjsr

Optimization of Heavy Metals Removal from Wastewater by Adsorption onto *Theobroma cacao* pod

[*1] Sanusi K. A., [2]Hammed A.M. and [3]Sanusi Q. K.
[1]Department of Chemical Sciences, Federal University Kashere, P.M.B. 0182, Gombe State, Nigeria.
[2]Department of Chemistry, University of Ilorin, Kwara State, Nigeria.
[3]Department of Microbiology, University of Ibadan, Oyo State, Nigeria.
*__Corresponding Author__: sanusikabir84@gmail.com; +2348060465459

Abstract:
In this study, *Theobroma cacao* pod (TCP) adsorbent was prepared, characterized and tested for removal of Cd^{2+} and As^{3+} from synthetic wastewater. The TCP had a good cation exchange capacity, large surface area and small particle size. The optimization results from Central Composite Design (CCD) predicted the adsorption percentages of 98.72 and 92.48 for Cd^{2+} and As^{3+} respectively. The experimental results revealed the removal percentages of Cd^{2+} and As^{3+} by TCP as 98.80% and 92.46% respectively, which were in good correlation with the values predicted by the CCD for the respective metal ions at the optimum conditions of adsorption. The isotherm studies showed that the adsorption of Cd (II) and As (III) ions onto TCP best fitted the Langmuir isotherm model. The kinetic studies showed that rate of adsorption of Cd (II) and As (III) ions followed the pseudo second- order kinetic model. Thermodynamic studies revealed that metal adsorption onto TCP was feasible, spontaneous and endothermic for Cd (II) ions while the uptake of As (III) followed an exothermic process. The TCP, owing to its good cation exchange capacity, low-cost and eco-friendliness, has a good potential to be utilized as an alternative adsorbent in wastewater treatment.

Keywords: Adsorption, experiment, isotherms, kinetics, thermodynamics
Received: 10th Sept, 2025 *Accepted:* 28th Nov, 2025 *Published Online:* 27th Dec 2025

Introduction

The principal objective of wastewater treatment is to allow municipal and industrial effluents to be disposed off without danger to human health or unacceptable damage to the natural environment and ecosystems (Utomo and Salim, 2008). Heavy metals are one of the most problematic pollutants in the environment due to their toxicity, persistence and bio-accumulation potentials. Direct toxicity to man and other forms of life and indirect toxicity through the food chains are the focus of this concern (Sanusi *et al*., 2021). Heavy metals such as cadmium, lead, chromium, arsenic and copper are released into the water bodies from several industrial activities such as mining, electroplating, battery manufacture, metallurgy and tannery. The effluents released from the industries contain heavy metals at a concentration above the tolerable limit (Ogbu *et al.*, 2019). In order to maintain a healthy living, essential metals such as Cu, Fe, Zn and Mn are required as micro-nutrients or macro-nutrients. However, other metals like Cd, Pb and As are poisonous; increased exposure to these metals can be hazardous as they damage nerves, brain, liver, heart, lung, bones and cause gastrointestinal dysfunction (Sanusi *et al.*, 2021).
To alleviate the problem of water pollution by heavy metals, various conventional methods including coagulation, floatation, adsorption,

ion exchange, reverse osmosis, ultrafiltration, electro-dialysis and membrane filtration processes have been used. However, most of these water treatment methods suffer several techno-economic limitations such as inefficiency, cost expensive, sludge production, membrane filters scarcity (Utomo and Salim, 2008). Removal of toxic chemical substances by adsorption using low-cost adsorbents is the latest method of choice in wastewater treatment. Among available natural materials, agricultural wastes are regarded as suitable adsorbents because they are non-toxic, abundant, eco-friendly and have multifunctional group properties. Several researchers have utilized a wide variety of agro-wastes for heavy metals removal in aqueous solutions. These include agrowastes such as pineapple leaves (Amphol *et al.*, 2020), Sawdust (Ogbu *et al*., 2019), *Carica papaya* seed (Sanusi *et al*., 2016), tiger nut (Sanusi *et al*., 2018) and mango seed (Olu-Owolabi *et al.*, 2012). *Theobroma cacao* pod (TCP) is the main by-products of cocoa processing discarded as wastes, constituting environmental pollution. *Theobroma cacao* pod (TCP) is a lignocellulosic waste consisting of cellulose 26.1%, hemicellulose 12.8% and lignin 28% (Sanusi *et al*., 2021). This study aims to investigate the isotherms, kinetics and thermodynamics of adsorption of Cd (II) and As (III) ions on *Theobroma cacao* pod from wastewater.

Material and Methods

Collection and pre-treatment of Adsorbent samples.

Theobroma cacao pods (TCP) were collected from cocoa plantations in Ifetedo town, Osun State. The TCP samples were washed with tap water and then rinsed with distilled water to remove dust, dirt impurities, oven-dried at 70C for 72 h and ground to powder using mortar and pestle. The TCP was sieved in a 0.230 mm sieve and stored plastic container (Olu-Owolabi *et al*., 2012).

Characterization of adsorbents

The cation exchange capacity (CEC) of TCP was determined using the ammonium acetate method as reported by Unuabonah *et al*. (2013). Na^+ and K^+ were determined using AES (Agilent PG 10T), while Ca^{2+} and Mg^{2+} were determined by atomic absorption spectrophotometer (SHIMAZU 360H Model). The functional groups present in the adsorbents were obtained using Shimadzu 8400S FTIR spectrometer (Adebowale *et al.*, 2008). The surface morphology, surface area and porosity of the adsorbent were analyzed using scanning electron microscopy (SEM), Philips XL30 model and Brunauer, Emmet and Teller (BET) (Singh and Bhateria, 2020).

Preparation of Synthetic Wastewater

Stock solutions of the metal ions (Cd^{2+} and As^{3+}) were prepared by dissolving 2.711g of $Cd(NO_3)_2$ and 1.320 g of As_2O_3 salts in 200 cm^3 deionized water and then made up to the mark in a 1000 cm^3 volumetric flask respectively. Working solutions of various concentrations of the heavy metals were prepared from the stock solution as required for the adsorption experiment.

Adsorption studies

Adsorption experiments were carried out in 100 cm^3 plastic bottles by contacting 1.5 g of adsorbent with 20 cm^3 of wastewater containing 100 mg/L each of Cd^{2+} and As^{3+}. The adsorbent/metal ions mixtures were placed on a rotary shaker and shaken at 120 rpm at a room temperature (300 K) for a period of 120 min to attain equilibrium (Ogbu *et al*., 2019). The sample mixtures were filtered using whatman 0.45 filter paper and the filtrates were analyzed for the concentration of the metal ions left using AAS method (Unuabonah *et al.*, 2013; Gusain *et al.*, 2019). All adsorption experiments were carried out in triplicate for all the metal ions studied.

Optimization of Adsorption Parameters

The central composite design (CCD) and Design-Expert 12 software was applied to determine the optimum set of adsorption parameters as presented in Table 1.

Table 1: Parameters for optimization of adsorption of Cd (II) and As (III) on TCP adsorbent

Independent variables	Ranges and Coded Levels				
	- α	-1	0	+1	+ α
Initial metal conc. (C_0) (mg/L)	50	75	100	125	150
pH	2	3	5	6	8
Adsorbent dose (D) (g)	0.5	1	1.5	2	2.5
Contact time (T)(min)	30	60	120	180	210

Model for determination of effect of interaction of adsorption parameters

A quadratic model in the form of expression below was developed for the adsorption of the metal ions as it was influenced by the adsorption parameters considered during the experiments. The response model may be represented as Equation 1:

$$Y = \beta_0 + \sum_{i=1}^{n} \beta_i X_i + (\sum_{i=1}^{n} \beta_{ii} X_i)^2 + \sum_{i=1}^{n} \sum_{j=i+1}^{n} \beta_{ij} X_i X_j + \varepsilon \quad (1)$$

Where, Y is the response, which is to be optimized the response (Y). β_0 is the intercept coefficient, β_i is the linear coefficients, β_{ii} is the quadratic coefficients, β_{ij} is the interaction coefficients, and X_i and X_j are the coded values of the independent process variables.

Data Treatment

The amount of metal ions adsorbed per gram of TCP was calculated using Equation 2.

$$q_e = \frac{(C_O - C_e)V}{M} \quad (2)$$

The percentage removal of metal ions by TCP was calculated using Equation 3.

$$\%R = \frac{C_o - C_e}{C_o} \text{ x } 100 \quad (3)$$

where; R is the removal efficiency of the metal ions by adsorbent; C_o is the initial metal ions concentration in wastewater (mg/L); C_e is the metal ions concentration adsorbed by an adsorbent at equilibrium (mg/L); q_e, V and M are the amount of metal ions adsorbed (mg/g), volume of the solution (mL) used for experiment and mass (g) of the sample, respectively.

Adsorption Isotherm Models

The equilibrium isotherm modeling of Cd^{2+} and As^{3+} adsorbed onto the TCP adsorbent was carried out by the application of the Langmuir and Freundlich models.

The Langmuir isotherm is represented in linear form by Equation 4 as:

$$\frac{C_e}{q_e} = \frac{1}{Q_o b} + \frac{C_e}{Q_o} \quad (4)$$

When $\frac{C_e}{q_e}$ is plotted against C_e, the slope is $\frac{1}{Q_o}$ and the intercept is $\frac{1}{Q_o b}$. Where Q_o and b are the maximal adsorption capacity per weight of TCP and solute-surface interaction energy parameters.

The Freundlich isotherm in linear form is represented by Equation 5 as:

$$\log q_e = \log K_F + \left(\frac{1}{n}\right)\log C_e \quad (5)$$

Where K_F and n are the Freundlich model capacity factor and the linearity parameter respectively. The values of K_F and n may be calculated by plotting log (q_e) versus log (C_e). The slope is equal to $\frac{1}{n}$ and the intercept is equal to $\log K_F$ (Unuabonah *et al*., 2008; Das and Mondal, 2011).

Adsorption Kinetic Models

The Lagergren pseudo-first-order (PFO) and pseudo second-order (PSO) kinetic models were employed in describing the rate of the metal adsorption process.

The Equations are expressed below:

PFO:
$$\log(q_e - q_t) = \log q_e - \frac{k_1}{2.303}t \quad (6)$$

PSO:
$$\frac{t}{q_t} = \frac{1}{k_2 q_e^2} + \frac{t}{q_e} \quad (7)$$

Where q_e and q_t are adsorption quantity (mg/g) at equilibrium and at time t, respectively; k_1 (min^{-1}) and k_2 (g/mg^1min^1) are the rate constants of the PFO and PSO, respectively. The q_e and rate constants were calculated from the slope and intercept of the plots of log $(q_e - q_t)$ *vs.* t; t/q *vs.* t and for PFO and PSO respectively (Adebowale *et al*., 2008, Sanusi *et al*., 2016).

Equilibrium Adsorption Analysis

A good statistical tool for evaluating the applicability and fitness of isotherm or kinetic models besides the regression coefficient (R^2) is the non-linear chi-square test (X^2). It is expressed as:

$$X^2 = \frac{(q_e exp - q_e cal)^2}{q_e cal} \quad (8)$$

Where, q_e exp (mg/g) and q_e cal (mg/g) are the experimental and calculated equilibrium adsorption capacities respectively. The smaller the X^2 value, the closer the agreement between the experimental data and data calculated from the model equations (Akpomie and Dawodu, 2015).

Thermodynamic parameters

The thermodynamic parameters, i.e. standard enthalpy change (ΔH^o), standard entropy change (ΔS^o), standard Gibbs free energy change (ΔG^o) and equilibrium constant (K_C) were evaluated using data from equilibrium metal adsorption studies through the following Equations:

$$K_C = \frac{C_{ads}}{C_e} \quad (9)$$

$$\Delta G^o = -RTInK_C = \Delta H^\circ - T\,\Delta S \quad (10)$$

$$\log K_C = -\frac{\Delta H^o}{2.303RT} + \frac{\Delta S^o}{2.303R} \quad (11)$$

Where C_{ads} and C_e are the amount of metal ions adsorbed and the amount left in solution after equilibrium; R and T are the universal gas constant (8.314 $Jmol^{-1}K^{-1}$) and temperature respectively.

Results and Discussion

Characterization of adsorbent.

The pH, cation exchange capacity (CEC), specific surface area and particle size of the TCP were presented in Table 2. The pH of TCP was measured as 7.60 ± 0.36 while its CEC was recorded as 56.80 ± 0.24 meq/100g. The specific surface area and particle size of the TCP adsorbent were calculated as 153.6 ± 0.10 m^2/g and 217.6 ± 0.12 µm respectively. From the results in Table 2, it was observed that the slightly basic pH of TCP has enhanced its adsorption capacity towards the metal ions uptake. The high specific surface area would practically expand the adsorptive capacity of the adsorbent. The small particle size of TCP suggests that the low-cost adsorbent possess the good adsorptive performance for the heavy metals (Sanusi *et al.*, 2021).

Table 2: Physicochemical characteristics of the TCP adsorbent.

Adsorbents	**pH**	**Exchangeable cations (meq/100g)**	**Specific surface Area (m^2/g)**	**Particle size (µm)**
TCP	7.60 ± 0.36	56.80 ± 0.24	153.6 ± 0.10	217.6 ± 0.12

The infrared spectra of TCP was presented in Figure 1. FTIR spectra of TCP exhibit a broad and strong −OH band at 3479 cm^{-1} indicating the presence of hydroxyl, phenolic or carboxylic −OH stretching vibration, typical of cellulose and lignin (i.e. free hydroxyl groups in the polysaccharide structure of its wall). The peak at about 3408 cm^{-1} is a −N−H stretching indicative of vibration associated with N- substituted amide (Sanusi *et al*., 2021). The two sharp absorption peaks at 2923 and 2854 cm^{-1} showed the presence of C–H stretch likely from aliphatic (methyl and methylene) groups. The sharp band appearing at 1747cm^{-1} is characteristic of typical C=O stretch bond from either a free acid or esterified carboxyl group. However, a distinct absorption band at 1651 cm^{-1} is assigned to a C=O stretching vibration of carbonyl group. The peak appearing around 1057 cm^{-1} is associated with the C−O bond or −C−C− stretching such as glycosidic linkage which are characteristic of polysaccharides. Similar observations have been reported by Pehlivan *et al.* (2007), Olu-Owolabi *et al.* (2012), and Unuabonah *et al*. (2013).

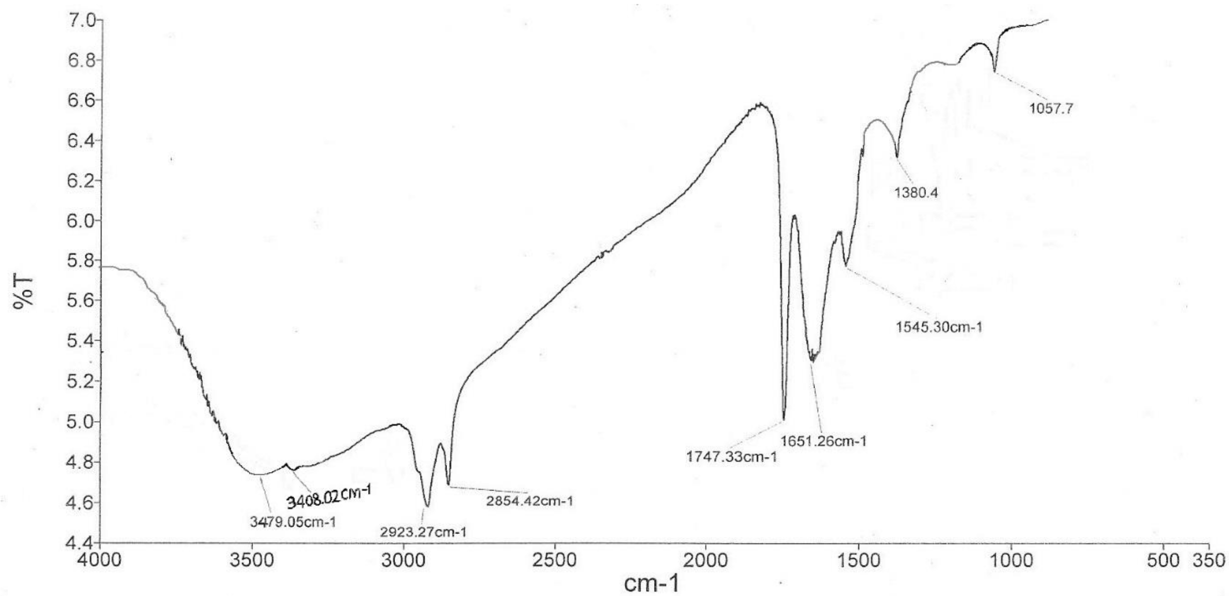

Figure 1. FTIR spectra of *Theobroma cacao* pod adsorbent (TCP).

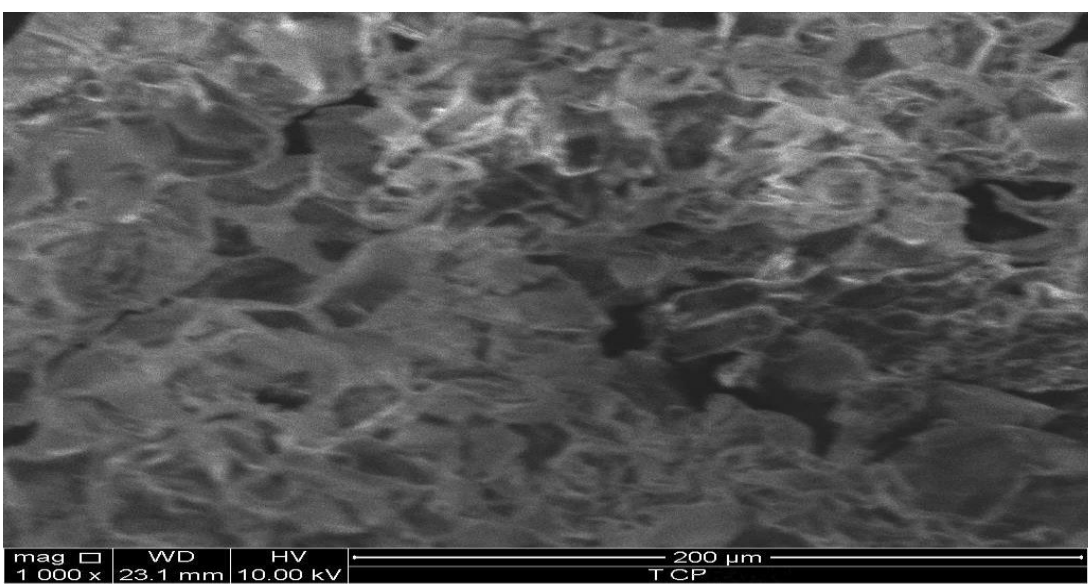

Figure 2: Scanning Electron Micrograph of TCP.

Figure 2 shows SEM micrographs of TCP. The adsorbent is porous, consists of a considerable number of heterogeneous pores, irregularly rough surface and aggregate of pore size and shapes typical of plant material (Olu-Owolabi *et al*., 2012). The TCP adsorbent showed the moderate pore sizes i.e. mesopores. Similar results have been reported by (Ogbu *et al.*, 2019; Sanusi *et al*., 2016).

Effect of adsorption parameters and optimization.

Table 3 presented the combined effect of interaction of pH, metal concentration, contact time and adsorbent dosage on the adsorptive behaviour of Cd (II) and As (III) onto TCP adsorbent. For the two metal ions, the adsorption increased with adsorbent dosage (1.5g), and this could be due to the presence of more active adsorption sites and large adsorbent's surface area that is readily available for metal uptake (Adebowale *et al*., 2008; Sanusi *et al.,* 2016). The removal of metal ions onto TCP reached the maximum at 120 min for Cd^{2+} and As^{3+}. Furthermore, the metal adsorption onto TCP depends on pH of the solution. High percentage Cd^{2+} and As^{3+} were adsorbed by TCP at pH 5 and pH 6 respectively as shown in Table 3, this is due to reduced or no competition between the metal ions and H^- in the aqueous solution. Similar observations were reported by other researchers (Ozde *et al.*, 2011; Yazdani *et al.*, 2014, Sanusi *et al*., 2021). As shown in Table 3, the optimization results using central composite design (CCD) revealed that the predicted adsorption capacities and percentages for the heavy metal ions (Cd^{2+} and As^{3+}) were close to the experimental values of the respective metal ions at the optimum conditions of adsorption parameters

.

Table 3. Optimization results for predicted and experimental values of adsorption capacity and percentages of Cd^{2+} and As^{3+} onto TCP adsorbent.

Heavy Metals	pH	Time (min)	Dose (g)	conc. (mg/L)	Adjusted R^2	Predicted R^2	Adsorption (%)		Adsorption capacity (mg/g)	
							Exp.	Pred.	q_e exp.	q_e pred.
Cd^{2+}	6	120	1.5	100	0.9959	0.9981	98.80	98.72	16.88	16.90
As^{3+}	5	120	1.5	100	0.9919	0.9966	92.46	92.48	12.50	12.45

Adsorption Isotherm Studies

The equilibrium data obtained from the adsorption of Cd (II) and As (III) ions onto TCP were fitted to Langmuir and Freundlich isotherm models. All of the isotherm parameters, constants and regression coefficients were calculated from the linear equations of the isotherm model plots and presented in Table 4.The maximum Langmuir monolayer adsorption capacity, Q_o (mg/g), were 98.80 and 92.46 for Cd^{2+} and As^{3+} uptake by TCP respectively. It was observed that the maximum adsorption capacity for Cd^{2+} was the higher i.e. $Cd^{2+} > As^{3+}$. The higher adsorption of Cd^{2+} in comparison with As^{3+} suggests that the adsorbent surface acts as a base and invariably have a stronger affinity for Cd^{2+} which was adsorbed in a borderline acidic solution (pH 6). However, the Q_o value for Cd^{2+} was higher than the values reported by Unuabonah *et al*. (2013) and Ozdes *et al*. (2011). As shown in Table 4, the Langmuir isotherm model was best fitted to adsorption of Cd^{2+} and As^{3+} onto the adsorbents with R^2 greater than 0.99 and low X^2 values (0.416 and 0.073) respectively. The results suggests that the adsorption process might be attributed to monolayer adsorption onto a homogenous surface of the adsorbent. Similar observations were reported by Ozdes *et al*. (2011) and Akpomie and Dawodu (2015).

Table 4: Adsorption isotherm parameters of Cd^{2+} and As^{3+} adsorption onto TCP adsorbent

Isotherm/Metal	**Q_o (mg/g)**	**b (L/mg)**	**R^2**	**X^2**
Langmuir				
Cd (II)	98.80	0.084	0.9996	0.416
As (III)	92.46	0.064	0.9990	0.073
Freundlich				
	K_F	n	R^2	X^2
Cd (II)	30.75	1.262	0.8697	8.409
As (III)	8.916	2.577	0.8766	8.258

Key: TCP: *Theobroma cacao* pod Q_o = Maximal adsorption capacity per unit weight of adsorbent, b = Solute–surface interaction energy-related parameter, R^2 = Regression coefficient, K_F = Freundlich model capacity factor, n = Isotherm linearity parameter, X^2 = Chi square test.

Adsorption Kinetic Studies

The pseudo-first-order (PFO) and pseudo second-order (PSO) kinetic models were applied to investigate the rate of the heavy metals adsorption. The calculated parameters, constants, regression coefficients (R^2) and chi-square (X^2) test for the adsorption of Cd (II) and As (III) ions obtained from the kinetic models were presented in Table 5. Plots of the two kinetic models are shown in Figures 3 (a and b). From Table 4, the experimental data calculated from pseudo-second order (PSO) kinetic model for Cd^{2+} and As^{3+} have higher R^2 ($0.99 < R^2 \leq 1$) and very low X^2 values ranging from (0.108 – 0.112). The higher R^2 and lower χ^2 values obtained suggested that the pseudo-second-order kinetic model provided a better fit for Cd^{2+} and As^{3+} than the pseudo-first-order model. More so, the q_e cal (mg/g) and rate constants of Cd^{2+} were higher than that of As^{3+} suggesting that cadmium is more attracted to the TCP (higher affinity) at faster rate than the uptake of As^{3+} onto the adsorbent. Similar observations has been reported for metal adsorption studies by Sanusi *et al*. (2016), Gusain *et al.* (2019) and Amphol *et al*. (2020).

Table 5: Adsorption Kinetic Parameters for Cd^{2+} and As^{3+} Adsorption onto TCP.

Kinetic Model/Metal	**Parameters**			
Pseudo-first-order (PFO)	q_e cal (mg/g)	k_1 (min^{-1})	R^2	X^2
Cd (II) q_e exp (44.64 mg/g)	57.41	6.29 x 10^{-1}	0.8867	29.21
As (III) q_e exp (26.80 mg/g)	48.32	1.80 x 10^{-2}	0.8851	20.78
Pseudo-second-order (PSO)	q_e cal (mg/g)	K_2 (g/mgmin^{-1})	R^2	X^2
Cd (II) q_e exp (44.64 mg/g)	44.64	6.40 x 10^{-3}	1.0000	0.108
As (III) q_e exp (26.80 mg/g)	26.81	5.94 x 10^{-3}	0.9999	0.112

Key: TCP: *Theobroma cacao* pod, q_e exp = adsorption quantity at equilibrium, q_e cal = adsorption quantity from the plots, k_1 = rate constant of the PFO, k_2 = rate constant of the PSO, R^2 = correlation coefficient, X^2 = Chi square test.

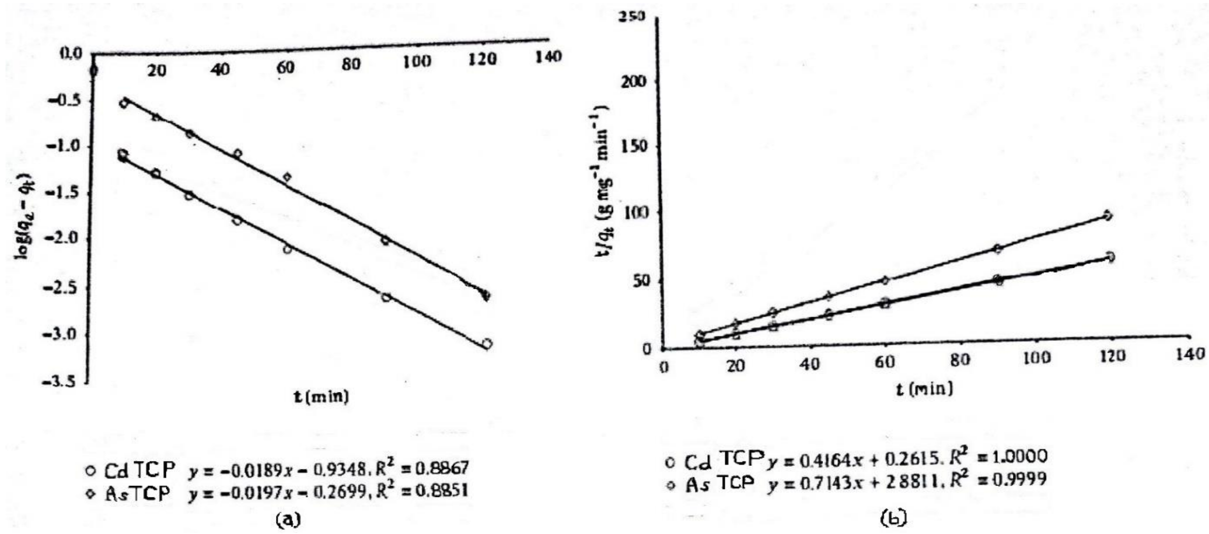

Figure 3: (a) PFO kinetic (b) PSO kinetic plots of adsorption of Cd (II) and As (III) onto TCP.

Thermodynamics of metal adsorption

The calculated values of the thermodynamic parameters for metal adsorption were given in Table 6. The Δ*G*° (kJmol^{-1}) values were negative for Cd (-2.34, -2.93) and As (-8.82, -4.78) at 308 and 328K respectively, suggesting the feasible and spontaneous adsorption of the metal ions onto TCP adsorbent. A similar observation has been reported for the adsorption Pb^{2+} and Cd^{2+} by Ozdes *et al*. (2011) and Dawodu and Akpomie (2014). The Δ*H*° (kJmol^{-1}) values for uptake of Cd onto TCP was +22.62 as shown in Table 6. The positive values of Δ*H*° indicated that Cd^{2+} uptake by the TCP was favourable at 308K, hence the adsorption process is endothermic (Mustapha *et al*., 2019; Ogbu *et al*., 2019). However, the negative values of Δ*H°* (kJmol^{-1}) was recorded for As (-14.71) suggesting the exothermic process of adsorption of As^{3+} onto the adsorbent surface (Rahman and Sathasivam, 2015; Sanusi *et al*., 2021). From Table 6, the Δ*H*° values for adsorption of Cd (II) onto the adsorbent 22.62 kJmol^{-1} suggestive of physicochemical adsorption process (Chukwuemeka-Okorie *et al*., 2018). However, the values of Δ*H*° for As^{3+} was -14.71 kJmol^{-1} respectively indicating physisorption (Ogbu *et al*., 2019). The positive Δ*S^0* values suggested the sorbent-solution interface's randomness during the adsorption of the metal ions onto the TCP. Similar observations have been reported by Mustapha *et al*. (2019) and Sanusi *et al*. (2021).

Table 6: Thermodynamic parameters for adsorption of Cd^{2+} and As^{3+} onto TCP.

Parameter/ Temperature (K)	Cd^{2+}	As^{3+}
Δ*H^0* (kJmol^{-1})	22.62	-14.71
Δ*S^0* (J/mol^{-1}K^{-1})	40.21	36.92
308K (Δ*G^0*)(kJmol^{-1})	-2.34	-8.82
318K (Δ*G^0*)(kJmol^{-1})	-2.51	-6.43
328K (Δ*G^0*)(kJmol^{-1})	-2.93	-4.78

Key: TCP: *Theobroma cacao* pod; Δ*H^0* = Change in standard enthalpy, Δ*S^0* = Change in standard entropy, and Δ*G^0* = Change in standard Gibbs free energy of metal adsorption.

Conclusion

In this research work, *Theobroma cacao* pod (TCP) adsorbent was prepared and tested for Cd^{2+} and As^{3+} removal from wastewater. The optimization results using central composite design (CCD) revealed that the predicted adsorption percentages of Cd^{2+} and As^{3+} were close to the experimental results of the respective metal ions at the optimum conditions of adsorption parameters. The isotherm studies showed that the adsorption of Cd^{2+} and As^{3+} onto TCP were best fitted to the Langmuir isotherm model. The kinetic studies revealed that the rate of adsorption of Cd^{2+} and As^{3+} followed pseudo-second order kinetic model. From thermodynamic studies, the metal adsorption process was feasible, spontaneous and endothermic for the case of Cd^{2+} while the uptake of As^{3+} was also feasible, spontaneous but exothermic. The results indicated that TCP had better adsorbent properties such as high cation exchange capacity, good adsorption performance and low-cost, hence an excellent adsorbent for heavy metals in wastewater management.

References

Adebowale, K.O., Unuabonah, I.E. and Olu-Owolabi, B.I. (2008). Kinetic and thermodynamic aspects of the adsorption of Pb^{2+} and Cd^{2+} ions on tripolyphosphate-modified kaolinite clay. *Chemical Engineering Journal*, 13(6): 99–107.

Akpomie, K.G. and Dawodu, F.A. (2015). Physicochemical analysis of automobile effluent before and after treatment with an alkaline-activated montmorillonite. *Journal of Taibah University for Science*, 9: 465–476.

Amphol, D., Napassorn, C., Kriangsak, S., Peerapan, D., Chalida, N. and Anusorn, S (2020). Removal of Heavy Metal Ions Using Modified Celluloses Prepared from Pineapple Leaf Fiber. *ACS Omega*, 5: 5285−5296.

Awala, H.A. and El Jamal, M.M. (2011). Equilibrium and kinetics study of adsorption of some dyes onto feldspar. *Journal of Chemical Technology and Metallurgy*, 46(1): 45-52.

Chukwuemeka-Okorie, H. O., Peter N. E., Akpomie K.G. and Olikagu, C.S. (2018). Calcined Corncob-Kaolinite Combo as New Sorbent for Sequestration of Toxic Metal Ions from Polluted Aqua Media and Desorption. *Frontiers in Chemistry*, 273(6): 1-13.

Gusain, Rashi., Neeraj, Kumar., Elvis, Fosso-Kankeu. and Suprakas, Sinha Ray (2019). Efficient Removal of Pb (II) and Cd (II) from Industrial Mine Water by a Hierarchical MoS2/SH-MWCNT Nanocomposite. *ACS Omega*, 4:13922−13935.

Md. Sayedur Rahman and Kathiresan V. Sathasivam (2015). Heavy Metal Adsorption onto *Kappaphycus* sp. from Aqueous Solutions: The Use of Error Functions for Validation of Isotherm and Kinetics Models. *BioMed Research International, Hindawi*, Pg 1-13.

Mustapha, S., Shuaib, D.T., Ndamitso, M. M., Etsuyankpa M. B. and Sumaila, A (2019). Isotherm, kinetic and thermodynamic studies for the removal of Pb (II), Cd (II), Zn (II) and Cu (II) ions from aqueous solutions using *Albizia lebbeck* pods. *Applied Water Sci*, 9:142.

Ogbu, I. C., Akpomie, K. G., Osunkunle A. A., and Eze, S.I. (2019). Sawdust-kaolinite composite as efficient sorbent for heavy metal ions. *Bangladesh J. Sci. Ind. Res.* 54(1): 99-110.

Olu-Owolabi, B., Oputu, O. U., Adebowale, K. O., Ogunsolu, O. and Olujimi, O. O. (2012). Biosorption of Cd^{2+} and Pb^{2+} ions onto mango stone and cocoa pod waste: Kinetic and equilibrium studies. *Scientific Research and Essays*, 7(15):1614-1629.

Olu-Owolabi, B.I, Alimoh H. Alabi, Emmanuel I. Unuabonah and Paul N. Diagboya (2016). Calcined bentonite-biomass composites for removal of aqueous metal ions. *Journal of Chemical and Engineering Technology*, 4:1379-1383.

Ozdes, D., Celal D. and Hasan, B. S. (2011). Adsorptive removal of Cd (II) and Pb (II) ions from aqueous solutions by using Turkish illitic clay. *Journal of Environ. Management*, 92: 3082-3090.

Sanusi, K.A., Babayo, A. U. and Isyaka, M. S. (2016). Evaluation of the Application of

Modified Feldspar Clay for Adsorption of Pb^{+2} and Cu^{+2} in Aqueous Media: Equilibrium and Thermodynamic studies. *Journal of Environmental & Analytical Toxicology*, 6(2): 02-09.

Sanusi, K. A., Yahaya, Y., Ambrusa, M. M., Rabiu, A. K. and Hammed, A. M. (2021). Optimization of Adsorption of Pb (II) and Cr (VI) from Aqueous Solution using Modified Feldspar Composite: Isotherm and Kinetic Studies. *International Journal of Engineering Science Technologies*, 5(4): 18–53.

Singh R. and Rachna B. (2020). Optimization and Experimental Design of the Pb^{2+} Adsorption Process on a Nano-Fe_3O_4-Based Adsorbent Using the Response Surface Methodology. *ACS Omega*, 5: 28305−28318.

Unuabonah, I.E., Olu-Owolabi, B.I., Adebowale, K.O. and Ofomaja, A.E. (2008). Adsorption of lead and cadmium ions from aqueous solutions by tripolyphosphate-impregnated kaolinite clay. *Journal of Colloids and Surfaces*, 82: 202-211.

Unuabonah, I.E., Olu-Owolabi, B.1., Andreas, Taubert and Adebowale. K.O (2013). SAPK: A Novel Composite Resin for Water Treatment with Very High Zn^{2+}, Cd^{2+} and Pb^{2+} Adsorption Capacity. *Industrial and Engineering Chemical Research*, 52: 578−585.

Utomo, Handojo Djati and Salim, Mohd Razman (2008). Adsorption of Heavy Metals from Water and Waste Water Using Low Cost Adsorbents from Agricultural By-Products. *Asian Journal of Water, Environment and Pollution*, 6(2): 73-80.

Yazdani, M., Bahrami, H. and Arami, M. (2014). Preparation and Characterization of Chitosan/Feldspar Biohybrid as an Adsorbent: Optimization of Adsorption Process via Response Surface Modeling. *The Scientific World Journal*, 20(14):1-13.